Korean Journal of Radiology

KJR

In Vitro and *In Vivo* Imaging of Prostate Cancer Angiogenesis Using Anti-Vascular Endothelial Growth Factor Receptor 2 Antibody-Conjugated Quantum Dot

Haejin Kwon, MS[1], Jiyeon Lee, PhD[1], Rita Song, PhD[1], Sung Il Hwang, MD[2], Junghan Lee, PhD[1], Young-Hwa Kim, MS[3], Hak Jong Lee, MD, PhD[2]

[1]Medicinal Chemistry Laboratory, Institute Pasteur Korea (IP-K), Seongnam 463-400, Korea; [2]Department of Radiology, Seoul National University College of Medicine, Seoul National University Bundang Hospital, Institute of Radiation Medicine, Seoul National University Medical Research Center, Clinical Research Institute, Seongnam 463-707, Korea;[3]Department of Nuclear Medicine and Biomedical Sciences Laboratory of Molecular Imaging and Therapy, Cancer Research Institute, Seoul National University College of Medicine, Seoul 110-744, Korea

Objective: Authors aimed to determine the targeting ability of vascular endothelial growth factor receptor 2 (VEGFR2)-conjugated quantum dots (QDs) in vitro, and apply it for a xenograft prostate cancer mouse model.
Materials and Methods: Conjugation reaction of QDs was performed by using the N-(3-dimethylaminopropyl)-N'-ethylcarbodiimide (EDC) and sulfo-(N-hydroxysulfosuccinimide) (Sulfo-NHS). The human umbilical vein cord endothelial cells (HUVECs) were incubated with QDs, conjugated with antiVGFR2, to see a specific binding *in vitro*. Fluorescent cell images were taken by a confocal microscope. The human prostate cancer cells (PC3) were injected to five nude mice on hind limbs to make the xenograft tumor model. QD-antiVEGFR2 antibody complex was injected into the tumor model and fluorescence measurements were performed at 1, 4, 9, 12, 15, and 24 hours after the injection.
Results: The specific interaction between HUVECs and QD-antiVEGFR2 antibody was clearly shown *in vitro*. The *in vivo* fluorescence image disclosed that there was an increased signal of tumor, 12 hours after the injection of QDs.
Conclusion: By showing endothelial cells binding with QDs-antiVEGFR2 antibodyand an experimental application of the antibody for VEGFR2 imaging in the prostate cancer xenograft mouse model, we suggests that the antibody-conjugated QDs can be a potential imaging tool for angiogenesis of the cancer.
Index terms: *Quantum dot; VEGFR2; Angiogenesis; Prostate cancer; Near infrared*

INTRODUCTION

Angiogenesis is the formation of new capillaries from existing blood vessels, and plays an important role for tumor growth and metastasis by providing oxygen and nutrients to the proliferating tumor cells (1-3). Moreover, the angiogenic activity is known to be related to tumor malignancy (4, 5). Therefore, angiogenic activity is highly relevant to the tumor state, and several probes were suggested to make a possible noninvasive detection. This strategy for tumor diagnosis may be expanded to monitoring of the tumor progression by drug treatment. Recently, the molecular imaging techniques have helped to develop a direct visualization and characterization of the cellular or molecular activation of angiogenesis-related phenomena (6). The role of the molecular imaging are becoming increasingly

important for studying this process, in both clinical and research settings, ranging from identifying the sites of angiogenesis to confirming the process of biochemistry that lies at the basis of the angiogenic process (7).

Quantum dots (QDs) are semiconductor nanocrystals with a quantum confinement property, which enables them to emit fluorescence from visible to infrared wavelengths on excitation (8). Over the last few years, due to their bright fluorescence, excellent photo-stability, and their narrow and tunable emission spectrum, QDs have gained much interest for biological imaging purposes (7).

Several specific endothelial molecular markers of angiogenesis are overexpressed on tumor vascular endothelial cells. Vascular endothelial growth factor receptor 2 (VEGFR2) is one of the major regulators of angiogenesis. Overexpression of VEGFR2 has been associated with tumor progression and poor prognosis in several tumors, including gastrointestinal tract, pancreas, breast, prostate, and lung cancers (9). Therefore, the imaging modalities, which can directly visualize specific molecular markers of angiogenesis, such as VEGFR2, would be very helpful for monitoring the angiogenic treatments and detection of the tumors.

The purpose of this study is to prepare antiVEGFR2 antibody, conjugated QDs, in order to confirm the targeting ability *in vitro*, and to evaluate the feasibility of the use of QDs in xenograft prostate cancer mouse models.

MATERIALS AND METHODS

Conjugation of AntiVEGFR2 Antibody to QDs

One nmol of antiVEGFR2 antibody (Santa Cruz Biotechnology Inc., Santa Cruz, CA, USA) was mixed with 10000 equivalent of N-(3-dimethylaminopropyl)-N'-ethylcarbodiimide (EDC, Sigma-Aldrich, St. Louis, MO, USA) and 12000 equivalent of sulfo-NHS (Molecular Bioscience, Boulder, CO, USA) in 0.1 M 2-(N-morpholino)ethanesulfonic acid buffer (pH 4.7, Pierce, Rockford, IL, USA). After incubation for 30 minutes at 25°C, the excess of reagents were removed by 50 k microcon centrifugal filter (Millipore, Billerica, MA, USA). The activated antiVEGFR2 antibody was then reacted with functionalized QD with amino PEG by the previously reported method (10) in 1 x phosphate buffered saline (PBS, Invitrogen, Eugene, OR, USA) for 3 hours at 25°C. Finally, both QDs530-antiVEGFR2 and QDs800-antiVEGFR2 conjugated were purified, using the Superdex® 200 size exclusion column (GE Healthcare, Pittsburgh, PA, USA), and have been characterized by an agarose gel

electrophoresis and dynamic light scattering (DLS). For the *in vitro* study, QDs530-antiVEGFR2 conjugates were used, and for the animal study, QDs800-antiVEGFR2 conjugates were used. The gel electrophoresis was run in a 0.5 x TBE buffer (Tris/borate/ethylenediaminetetraacetic acid, Sigma-Aldrich, St. Louis, MO, USA), using a 1% agarose gel at 50 V for 1 hour. To identify the QD-antibody conjugate, the gel was post-stained with colloidal blue solution. The number of VEGFR2 per QDs was determined by a bicinchoninic acid (BCA) protein assay (Thermo Scientific, Rockford, IL, USA).

HUVEC Cell Culture

Human umbilical vein cord endothelial cells (HUVECs) were purchased from company (Innopharma Screen, Asan, Korea). The cells were grown in M199 media, supplemented with penicillin-streptomycin 10 mL/L, 25 mM 4-(2-hydroxyethyl)-1-piperazineethanesulfonic acid (HEPES), 10 unit/ml Heparin, 2.2 g/L sodium bicarbonate, and 20% fetal bovine serum (FBS)/b-fibroblast growth factor 20 ng/mL.

In Vitro Cell Imaging Using QDs-AntiVEGFR2 Antibody

The interaction of QDs-antiVEGFR2 antibody with the cells was investigated, using a confocal fluorescence microscope (LSM 5 Live, Carl Zeiss, Oberkochen, Germany), as reported previously (11). HUVEC (10000 cells/well) were seeded in 8-well chambered cover glass (Lab-Tek, Thermo Scientific, Rochester, NY, USA) with 400 µL of cell media. After 24 hour incubation at 37°C, the cells were fixed by 4% paraformaldehyde (Wako, Osaka, Japan) for 20 minutes, and were washed by PBS, several times. A 150 nM of QDs530 and QDs530-antiVEGFR2 antibody conjugates were added to each well. They were incubated at 37°C for 3 hours. To remove the non-specific binding of QDs, the cells were washed by PBS and 0.01% tween20. Nucleus was stained by 4', 6-diamino-2-phenylindole (DAPI). For excitation of QDs, 488 Ar-ion laser was used with emission band pass filter of 495-555 nm, while the DAPI was excited with 405 nm laser and observed with emission band pass filter of 420-480 nm. A 40 x water objective was used for obtaining all of the fluorescent images and differential interference contrast (DIC) images.

PC3 Prostate Tumor Model

Five male Athymic nude mice of 6-7 weeks old were obtained from an animal facility (Orient, Seoul, Korea) and were housed under a specific pathogen-free environment.

The mice were maintained under controlled conditions (12-hour dark-light cycles; temperature, 20-24.8°C) with free access to sterilized mouse chow.

The PC-3 was purchased from the cell line bank (Korean Cell Line Bank, Seoul, Korea). The cells were grown in RPMI 1640 medium, supplemented with 10% FBS and penicillin-streptomycin. The cells were cultured at 37°C in a humidified 5% CO_2/95% air atmosphere.

To generate the tumor cells, prostate cancer cells (PC3) (1.5×10^6 cells in PBS 0.2 mL) was injected, subcutaneously, into the back or the right flank of the mice. After 4 to 6 weeks, tumors were allowed to grow to the mean maximum diameter of 15 mm (range, 10-15 mm). All animal protocols were approved by the Institutional Animal Care and Use Committee.

In Vivo Imaging of QDs and QDs-VEGFR2

Fluorescent images were obtained, using a Maestro *in vivo* Imaging System (CRi Inc., Woburn, MA, USA) for data acquisition and analysis. Before imaging, the mice were anesthetized by intraperitoneal injection of a solution containing 8 mg/mL ketamine (Ketalar®, Panpharma, Fougères, France) and 0.8 mg/mL xylazine (Rompun®, Bayer Pharma, Puteaux, France) at 0.01 mL/g of body weight.

QDs800-antiVEGFR2 antibody complex (140 pmole/mice) was injected via retro orbital route into three mice. Fluorescence measurements were performed at 1, 4, 9, 12, 15 and 24 hours after the injections. As a control group, control QDs800 without VEGFR antibody complex (140 pmole/mice) was injected into two mice.

In all cases, optical image sets were composed of a Cermax®-type 300 Watt Xenon lamp with a green filter set (a band-pass filter from 503 to 548 nm and 560 nm longpass filter, which were used for excitation and emission, respectively) to acquire one complete image cube. The tunable filter was automatically increased in 10-nm increments from 560 to 750 nm. A camera was used to capture the images at each wavelength, using a constant exposure. The system control was done with LabVIEW (National Instruments cooperation, Austin, TX, USA). The images were transferred to Image J software (http://rsbweb.nih.gov/ij/) as a JEPG format. The regions of interest (ROIs) were drawn on the tumor site, and the hind limb as a signal of background. This method was adapted from the other published study by Schellenberger et al. (12). We measured the ROI values three times from different locations, and the mean values were used for representative values.

After imaging, the mouse was sacrificed and the tumor tissue was prepared for VEGFR2 immunohistochemical staining. Immunostaining of VEGFR2 was performed using polymeric methods (DAKO real envision detection Systems, Glostrup, Denmark). The consecutive sections obtained from formalin-fixed specimen were made into paraffin-embedded blocks, and were deparaffinized. The rehydrated sections were boiled in a 0.01% sodium citrate buffer (pH 6.0), and then incubated with 3% hydrogen peroxide to block the endogenous peroxidase activity. The sections were then probed with monoclonal anti-VEGFR2 antibody (Santa Cruz Biotechnology, Inc., Santa Cruz, CA, USA). After incubation with horseradish peroxidase-labelled polymer, they were exposed to chromogen plus 3, 3'-diaminobenzidine substrate, and then counterstained with hematoxylin.

RESULTS

Figure 1 illustrates QDs-antiVEGFR2 antibody was synthesized using EDC chemistry. A gel electrophoresis analysis and DLS data of QDs-antiVEGFR2 antibody conjugates are shown in Figures 2, 3. The gel electrophoresis data showed that QDs were first modified with polyethylene glycol (PEG)-NH2, and anti VEGFR2 antibody was successfully conjugated with QDs-PEG-NH$_2$ as confirmed with colloidal blue staining. The hydrodynamic diameter of the resulting QDs-antiVEGFR2 antibody conjugate was much bigger than amine-functionalized QDs, which confirmed again that the antiVEGFR2 antibody was attached on QDs. From BCA protein assay (data is not shown here), the number of antiVEGFR2 antibody per QD was about 1.

Human umbilical vein cord endothelial cells were incubated with QDs530-antiVEGFR2 antibody and QDs530 to see a specific binding of QDs-antiVEGFR2 antibody conjugates in the endothelial cells, which express exclusively VEGFR2 on their membrane. Representative
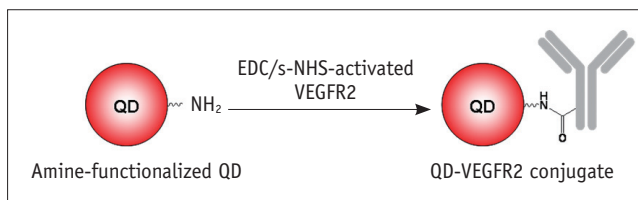
Fig. 1. Synthetic scheme for QD-VEGFR2 conjugate. Activated antiVEGFR2 antibody was reacted with functionalized QD with aminoPEG in 1 x phosphate buffered saline. QD = quantum dot, VEGFR2 = vascular endothelial growth factor receptor 2, PEG = polyethylene glycol
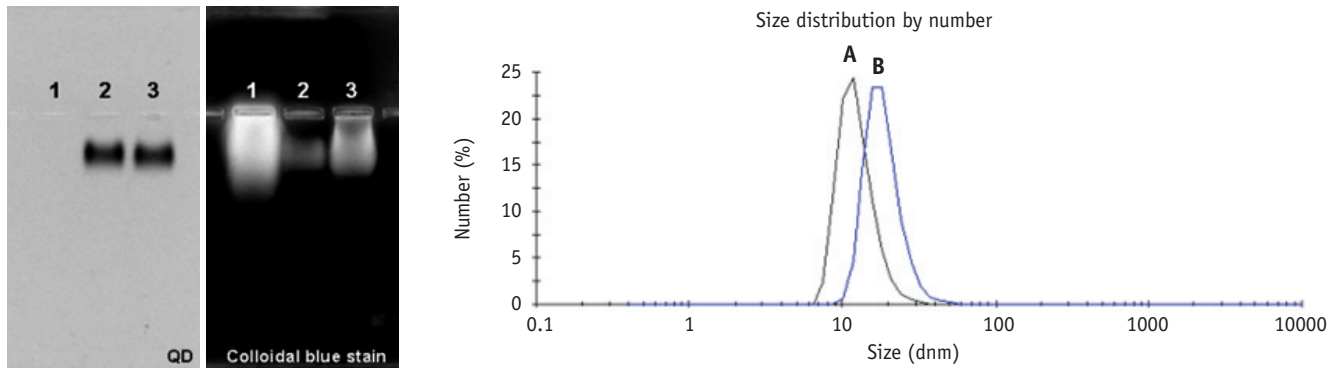
Fig. 2. Agarose gel electrophoresis of (1) EDC/s-NHS-activated VEGFR2, (2) QDs800-NH₂ and (3) QDs800-VEGFR2 conjugate.
DLS spectrum of **(A)** QDs800-PEG-NH₂ (12.6 ± 3.6 nm) and **(B)** QDs-VEGFR2 conjugate (18.7 ± 5.3 nm). EDC = N'-ethylcarbodiimide, DLS = dynamic light scattering, PEG = polyethylene glycol, VEGFR2 = vascular endothelial growth factor receptor 2, QDs = quantum dots, NHS = N-hydroxysulfosuccinimide
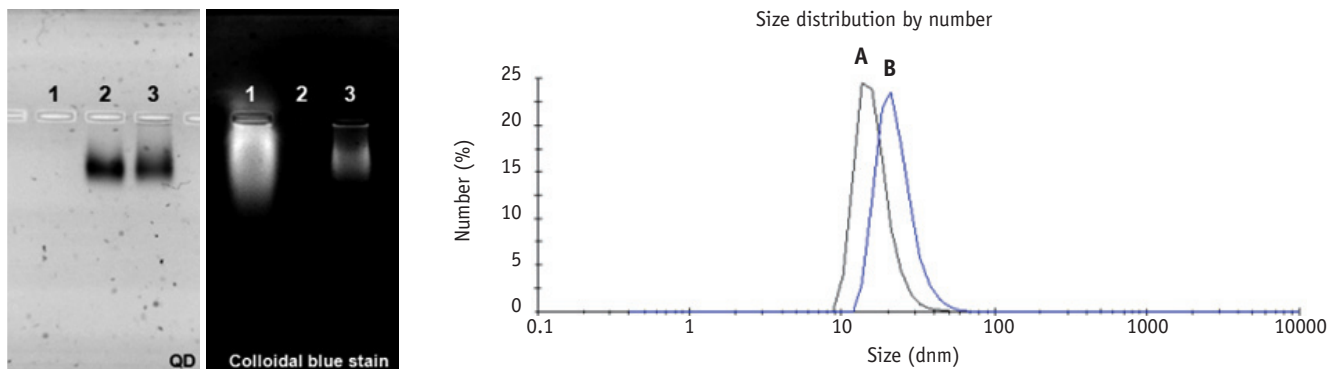
Fig. 3. Agarose gel electrophoresis of (1) EDC/s-NHS-activated VEGFR2, (2) QDs530-NH₂ and (3) QDs530-VEGFR2 conjugate.
DLS spectrum of **(A)** QDot530-PEG-NH₂ (16.1 ± 4.4 nm) and **(B)** QDs-VEGFR2 conjugate (22.7 ± 6.9 nm). EDC = N'-ethylcarbodiimide, DLS = dynamic light scattering, PEG = polyethylene glycol, VEGFR2 = vascular endothelial growth factor receptor 2, QDs = quantum dots, NHS = N-hydroxysulfosuccinimide

DIC and fluorescent images were shown in Figure 4. Green fluorescent QDs-antiVEGFR2 antibody was bound to HUVECs, whereas, QDs without the antibody were not observed in the cells. This result showed that there was a specific binding between HUVECs and QDs-antiVEGFR2 antibody.

Figure 5 shows serial fluorescent images after an injection of the antiVEGFR2 antibody conjugated QDs. The images showed that there is an increased signal of tumors after 12 hours of QDs injections. Figure 6 shows a signal to the background ratio, at each time point. As with the findings of optical imaging, the ratio is also increasing after 12 hours of QDs injections.

Figure 7 shows the immunohistochemical staining results of the tumor. There was positive staining of VEGFR2, which confirms that the tumor expressed the VEGFR2.

DISCUSSION

Angiogenesis, which is the formation of new functional blood vessels, plays an important role in many disease processes, including ischemia or cancer. Angiogenesis is a critical process in the tumor growth and invasion (13, 14). Many researches, investigating molecular pathways of tumor angiogenesis, have led to the identification of a number of key molecules that are involved in the stimulation of new vessel growth from existing host vasculature. Therefore, it is not surprising that many studies have focused on the angiogenic markers, such as VEGFR or $\alpha v \beta_3$ receptor (9) as a target for anti-angiogenic drugs.

Quantum dots are dot shape semiconductor particles with diameters on the order of 2-8 nm in visible fluorescent range, which roughly contains 200-10000 atoms. Due to their novel optical and electronic properties, QDs have been intensively studied as a new class of nano probe for molecular, cellular, and *in vivo* imaging (15, 16). Because the emission wavelength of QDs is size-dependent, fluorescence color may be fine-tuned throughout the visible and near infrared (NIR) spectrum, during a chemical
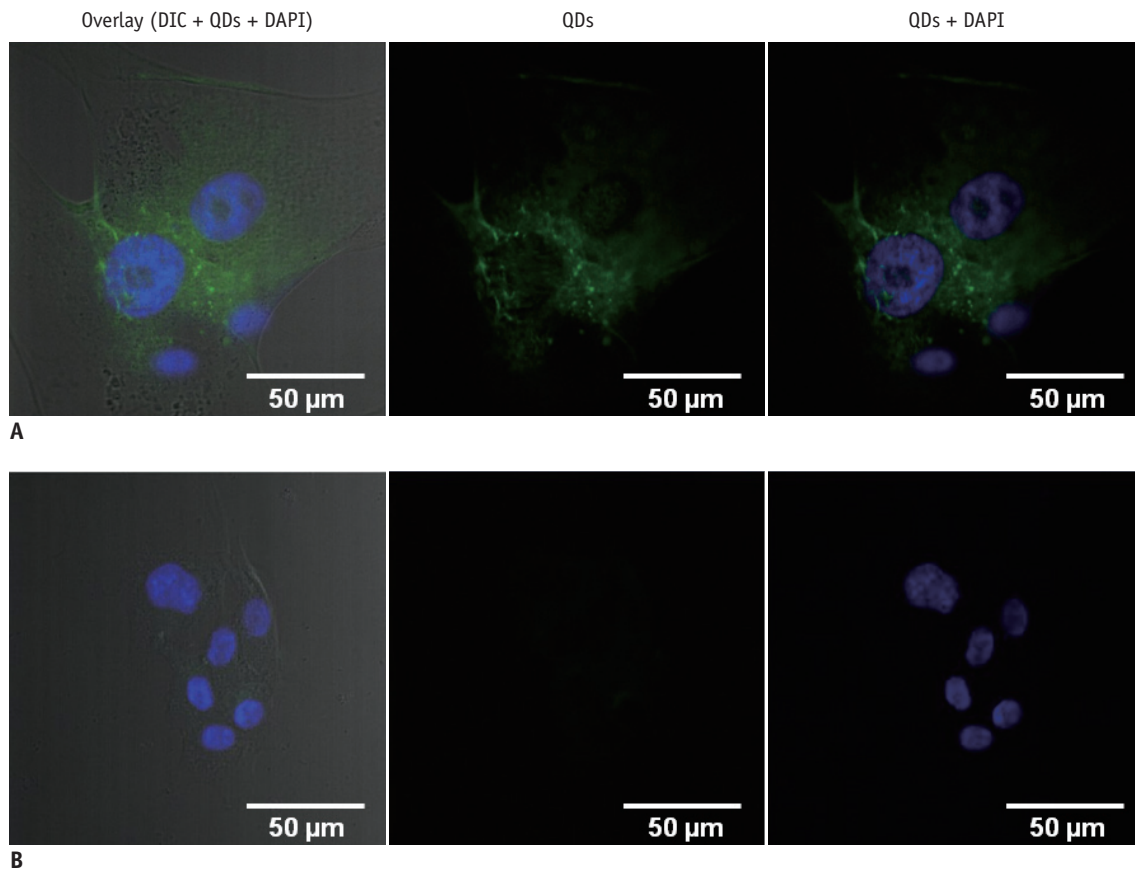
Fig. 4. Confocal microscope images of HUVEC interacted to QDs-VEGFR2 and QDs. Green fluorescence indicates QDs interaction to cells. QDs-VEGFR2 bound to HUVEC, while there was no QD binds to HUVEC without VEGFR2 conjugation.
A. HUVEC with QDs-VEGFR2. **B.** HUVEC with QDs only (left: overlaid image of DIC and fluorescent images, middle: green fluorescent [QDs] image, right: overlaid image of blue [DAPI] and green fluorescent images). HUVEC = human umbilical vein cord endothelial cells, DIC = differential interference contrast, DAPI = 4',6-diamidino-2-phenylindole, QDs = quantum dots, VEGFR2 = vascular endothelial growth factor receptor 2

synthesis, by controlling the QD size and composition. The semiconducting nature and the size-dependent fluorescence of QDs have made them very attractive for use in optoelectronic devices and biological detection. (15). In addition, QDs have a continuous absorption band and a narrow Gaussian emission profile. These combined properties enable excitation of multiple-colored QDs with a common excitation source and the detection of multiple colors within a limited spectral window without cross-talk (17).

Quantum dots conjugated with an antibody have been extensively studied because of their possible application in the bioimaging (11, 18-20). QDs conjugated with antiVEGFR2 antibody have also been studied by Chen et al. (18) for a dual-function positron emission tomography/near-infrared fluorescence probe. Although this research showed QD conjugated with antiVEGFR2 antibody and its application in tumor imaging, more detailed characterization and specific binding studies will be needed

to improve the potential of the QD-antibody conjugates in the area of tumor diagnostics.

The importance of the diagnosis and therapy of prostate cancer is increasing since prostate cancer has become a leading cause of morbidity and mortality in men. The evaluation of angiogenesis is also important in the development and spread of prostate cancer. Several studies have shown the importance of evaluation of tumor neovascularization, because it was definitely correlated with an increased risk of distant metastasis and prostate cancer recurrence after surgery, as well as with poorer overall survival (21, 22).

The targeted delivery of biocompatible QD conjugates *in vivo* has been limited to date to detect specific vascular biomarkers in the tissue. Gao et al. (23) used QDs conjugated to monoclonal antibodies directed against prostate-specific membrane antigen to target and image human prostate cancer cells, which are growing in the liver of mice. More recently, arginine-glycine-aspartic acid
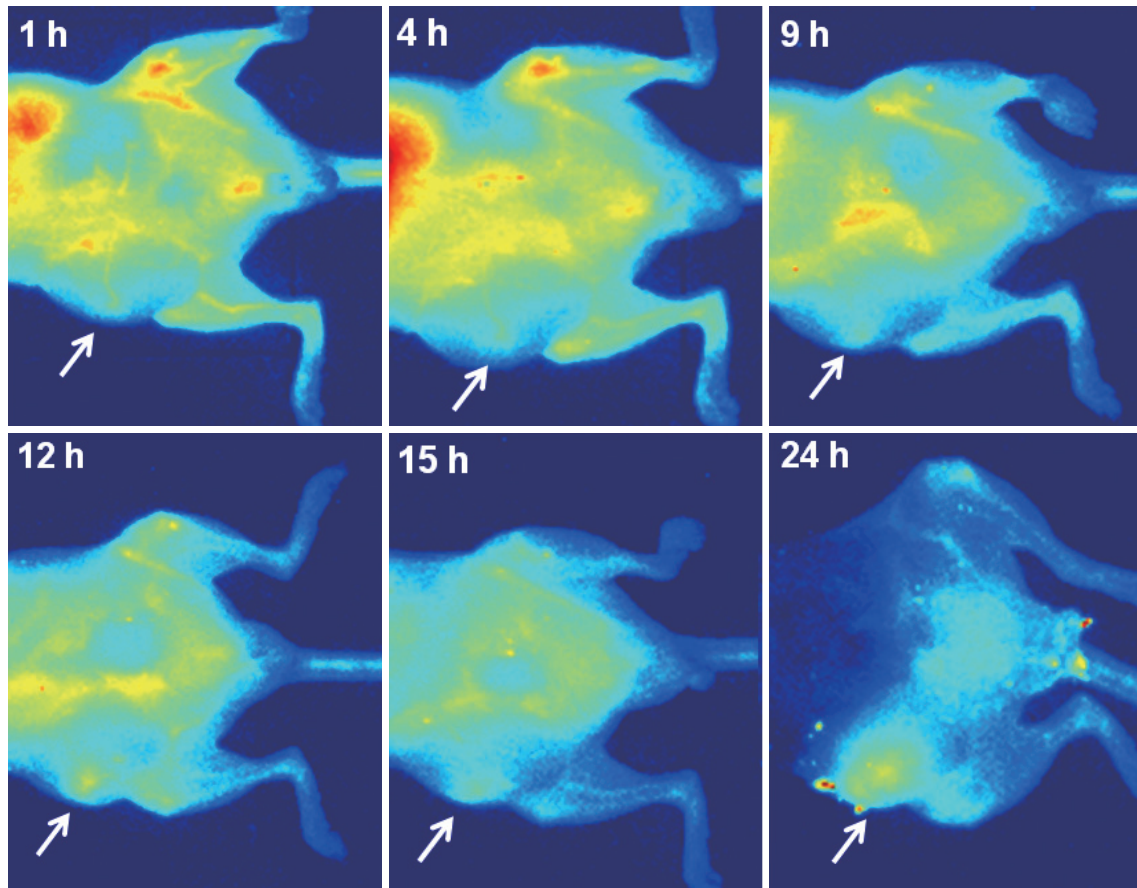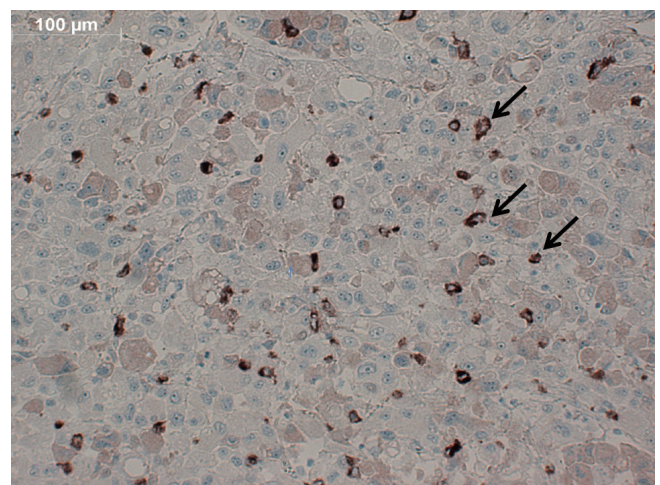
Fig. 5. *In vivo* fluorescent images after vascular endothelial growth factor receptor 2 targeted near infrared quantum dot injection (after 1 hour, 4 hours, 9 hours, 12 hours, 15 hours, 24 hours). Signal from tumor is apparent since 12 hours after injection (arrows).
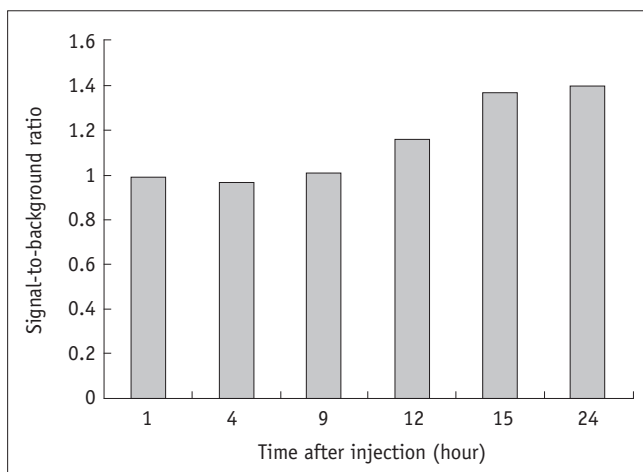
Fig. 6. Ratio of signals of tumor to background signal. Graph shows that ratio is increasing after 12 hours after quantum dot injections.

Fig. 7. Immunohistochemical staining of VEGFR2 of tumor specimen. Slide shows relatively definite staining of VEGFR2, which confirms that tumor expressed VEGFR2 (arrows). VEGFR2 = vascular endothelial growth factor receptor 2

peptide-conjugated QDs have been used to specifically target integrin $\alpha v \beta_3$ in a murine xenograft model because the integrin $\alpha v \beta_3$ is significantly upregulated in the tumor, but not in the normal tissue (17, 24, 25).

In our study, we used NIR QDs for *in vivo* imaging studies. One of the greatest advantages of QDs for imaging in living tissue is that their emission wavelengths can be

tuned throughout the NIR spectrum, by adjusting their composition and size, resulting in photostable fluorophores that are stable in biological buffers (16). The superiority of NIR QDs has been demonstrated in sentinel lymph node mapping, a common procedure in breast cancer surgery, whereby, the lymph node closest to the organ affected is monitored for the presence of locally disseminated cancer cells (17). However, despite those advantages of NIR emission, locating the fluorescent objects *in vivo* can still be challenging because tissue absorption and scattering, in addition to limiting the light coming out of the subject, also limit the amount of incident excitation light that reaches the fluorophores. To the best of our knowledge, there is no report regarding imaging of the prostate tumor angiogenesis, using NIR QDs.

With the exciting potential of QDs for clinical application, the potential toxicity of QDs has become a serious concern. Theoretically, the toxicity of QDs can be derived from the leakage of toxic core semiconductor materials (such as CdSe/ZnS), by UV irradiation, and nonspecific uptake through endocytosis, inducing cell apoptosis and the transfer of absorbed optical energy to nearby oxygen molecules, generating reactive oxygen species (ROS) (26-28). It may be of greater concern that QDs, and many other types of nanoparticles, have been found to aggregate, bind nonspecifically to cellular membranes and intracellular proteins, and induce the formation of ROS (15).

In our study, the images of HUVECs showed the targeting ability of QD-antibody conjugates with a specific binding between QDs-antiVEGFR2 and the cells. As shown on Figure 4, confocal microscope images of HUVEC revealed that HUVEC cells with QDs-VEGFR2 showed strong interactions, whereas, the HUVEC with QDs only showed no signals. Our results suggest that we can selectively visualize the cells with high activity of VEGFR2, which can suggest the potential for the diagnosis or therapy onto the specific cells. However, the binding to VEGFR2 cannot be tumor-specific binding, as it can be shown in any tumors that have increased level of VEGFR2 or other conditions with increased VEGFR2.

There are several reports for imaging the angiogenesis in animal and clinical studies (29-31). Jun et al. (29) tried to visualize the tumor angiogenesis using a VEGF receptor 2 antibody conjugated magnetic resonance contrast agent, and Ko et al. (30) evaluated angiogenesis using an ultrasound contrast agent, using animal models. In a clinical study, Kim et al. (31) compared the perfusion parameters in CT with tumor grade and microvessel density.

The *in vivo* images revealed that there were increased signals from tumors comparing with the surrounding tissues, after 12 hours after injection (Fig. 5). Our findings from *in vitro* and *in vivo* images suggest the possibilities that these targeting QDs could be used in living objects, even though many tremendous studies, regarding the optimal dose, toxicity, and biodistribution would be needed.

The main limitation of our study is that the number of *in vivo* cases is too small to analyze statistically. Out of the five animals used in our study, only one case survived and showed QD signals from tumors, despite its possibilities of NIR QDs *in vivo*. The remaining four animals were dead during imaging after intraperitoneal anesthesia. We think one of the main reasons is due to the temperature, because there was no heater or warm bed in the chamber of fluorescent imaging system we used. The nude mouse are very vulnerable to the temperature changes or other stress, so caring them required more experience and knowledge concerning caring nude mouse models. The other possibilities include the toxicity of QD. For clinical application of NIR QD, the safety issue needs to be evaluated, thoroughly. Even though the *in vivo* results are unsatisfactory, we could show the possibilities for imaging tumor in living object with NIR QD from our results from an *in vivo* study. Further studies, using animal models, would be needed for detailed evaluation in the living object.

In spite of these limitations, we tried to get *in vitro* and *in vivo* images regarding VEGFR2 using QDs, which is one of the most potential nanomaterials for molecular imaging.

In conclusion, we showed that the endothelial cells were labeled by QDs-antiVEGFR2 antibody with the specific binding, and *in vivo* image of the prostate cancer xenograft mouse model indicated a potential application for VEGFR2 imaging *in vivo*. This approach suggests that antibody conjugated QDs can be a promising detector of cancer angiogenesis in the field of tumor diagnosis.

REFERENCES

1. Folkman J. Tumor angiogenesis: therapeutic implications. *N Engl J Med* 1971;285:1182-1186
2. Oostendorp M, Douma K, Hackeng TM, Dirksen A, Post MJ, van Zandvoort MA, et al. Quantitative molecular magnetic resonance imaging of tumor angiogenesis using cNGR-labeled paramagnetic quantum dots. *Cancer Res* 2008;68:7676-7683
3. Carmeliet P. Angiogenesis in health and disease. *Nat Med* 2003;9:653-660
4. Meitar D, Crawford SE, Rademaker AW, Cohn SL. Tumor

angiogenesis correlates with metastatic disease, N-myc amplification, and poor outcome in human neuroblastoma. *J Clin Oncol* 1996;14:405-414

5. Daldrup H, Shames DM, Wendland M, Okuhata Y, Link TM, Rosenau W, et al. Correlation of dynamic contrast-enhanced MR imaging with histologic tumor grade: comparison of macromolecular and small-molecular contrast media. *AJR Am J Roentgenol* 1998;171:941-949

6. Massoud TF, Gambhir SS. Molecular imaging in living subjects: seeing fundamental biological processes in a new light. *Genes Dev* 2003;17:545-580

7. Mulder WJ, Castermans K, van Beijnum JR, Oude Egbrink MG, Chin PT, Fayad ZA, et al. Molecular imaging of tumor angiogenesis using alphavbeta3-integrin targeted multimodal quantum dots. *Angiogenesis* 2009;12:17-24

8. Zhang H, Yee D, Wang C. Quantum dots for cancer diagnosis and therapy: biological and clinical perspectives. *Nanomedicine (Lond)* 2008;3:83-91

9. Willmann JK, Paulmurugan R, Chen K, Gheysens O, Rodriguez-Porcel M, Lutz AM, et al. US imaging of tumor angiogenesis with microbubbles targeted to vascular endothelial growth factor receptor type 2 in mice. *Radiology* 2008;246:508-518

10. Yang YA, Wu H, Williams KR, Cao YC. Synthesis of CdSe and CdTe nanocrystals without precursor injection. *Angew Chem Int Ed Engl* 2005;44:6712-6715

11. Lee J, Choi Y, Kim K, Hong S, Park HY, Lee T, et al. Characterization and cancer cell specific binding properties of anti-EGFR antibody conjugated quantum dots. *Bioconjug Chem* 2010;21:940-946

12. Schellenberger EA, Bogdanov A Jr, Petrovsky A, Ntziachristos V, Weissleder R, Josephson L. Optical imaging of apoptosis as a biomarker of tumor response to chemotherapy. *Neoplasia* 2003;5:187-192

13. Deshpande N, Pysz MA, Willmann JK. Molecular ultrasound assessment of tumor angiogenesis. *Angiogenesis* 2010;13:175-188

14. Hicklin DJ, Ellis LM. Role of the vascular endothelial growth factor pathway in tumor growth and angiogenesis. *J Clin Oncol* 2005;23:1011-1027

15. Smith AM, Duan H, Mohs AM, Nie S. Bioconjugated quantum dots for in vivo molecular and cellular imaging. *Adv Drug Deliv Rev* 2008;60:1226-1240

16. Kim S, Lim YT, Soltesz EG, De Grand AM, Lee J, Nakayama A, et al. Near-infrared fluorescent type II quantum dots for sentinel lymph node mapping. *Nat Biotechnol* 2004;22:93-97

17. Bentolila LA, Ebenstein Y, Weiss S. Quantum dots for in vivo small-animal imaging. *J Nucl Med* 2009;50:493-496

18. Chen K, Li ZB, Wang H, Cai W, Chen X. Dual-modality optical and positron emission tomography imaging of vascular

endothelial growth factor receptor on tumor vasculature using quantum dots. *Eur J Nucl Med Mol Imaging* 2008;35:2235-2244

19. Zhang H, Zeng X, Li Q, Gaillard-Kelly M, Wagner CR, Yee D. Fluorescent tumour imaging of type I IGF receptor in vivo: comparison of antibody-conjugated quantum dots and small-molecule fluorophore. *Br J Cancer* 2009;101:71-79

20. Chen LD, Liu J, Yu XF, He M, Pei XF, Tang ZY, et al. The biocompatibility of quantum dot probes used for the targeted imaging of hepatocellular carcinoma metastasis. *Biomaterials* 2008;29:4170-4176

21. Weidner N, Carroll PR, Flax J, Blumenfeld W, Folkman J. Tumor angiogenesis correlates with metastasis in invasive prostate carcinoma. *Am J Pathol* 1993;143:401-409

22. Schlemmer HP, Merkle J, Grobholz R, Jaeger T, Michel MS, Werner A, et al. Can pre-operative contrast-enhanced dynamic MR imaging for prostate cancer predict microvessel density in prostatectomy specimens? *Eur Radiol* 2004;14:309-317

23. Gao X, Cui Y, Levenson RM, Chung LW, Nie S. In vivo cancer targeting and imaging with semiconductor quantum dots. *Nat Biotechnol* 2004;22:969-976

24. Cai W, Chen K, Li ZB, Gambhir SS, Chen X. Dual-function probe for PET and near-infrared fluorescence imaging of tumor vasculature. *J Nucl Med* 2007;48:1862-1870

25. Cai W, Shin DW, Chen K, Gheysens O, Cao Q, Wang SX, et al. Peptide-labeled near-infrared quantum dots for imaging tumor vasculature in living subjects. *Nano Lett* 2006;6:669-676

26. Hardman R. A toxicologic review of quantum dots: toxicity depends on physicochemical and environmental factors. *Environ Health Perspect* 2006;114:165-172

27. Ipe BI, Lehnig M, Niemeyer CM. On the generation of free radical species from quantum dots. *Small* 2005;1:706-709

28. Lovrić J, Cho SJ, Winnik FM, Maysinger D. Unmodified cadmium telluride quantum dots induce reactive oxygen species formation leading to multiple organelle damage and cell death. *Chem Biol* 2005;12:1227-1234

29. Jun HY, Yin HH, Kim SH, Park SH, Kim HS, Yoon KH. Visualization of tumor angiogenesis using MR imaging contrast agent Gd-DTPA-anti-VEGF receptor 2 antibody conjugate in a mouse tumor model. *Korean J Radiol* 2010;11:449-456

30. Ko EY, Lee SH, Kim HH, Kim SM, Shin MJ, Kim N, et al. Evaluation of tumor angiogenesis with a second-generation US contrast medium in a rat breast tumor model. *Korean J Radiol* 2008;9:243-249

31. Kim JW, Jeong YY, Chang NK, Heo SH, Shin SS, Lee JH, et al. Perfusion CT in colorectal cancer: comparison of perfusion parameters with tumor grade and microvessel density. *Korean J Radiol* 2012;13 Suppl 1:S89-S97